Organic Electronics 13 (2012) 457–463

Contents lists available at SciVerse ScienceDirect

Organic Electronics

journal homepage: www.elsevier.com/locate/orgel

$Au^{I}\cdots Au^{I}$ interaction induced semiconducting microwires with photo- and vapor-responsive properties

Xiaoyue Mu, Dong Liu, Xiao Cheng, Lu Li, Hongyu Zhang *, Yue Wang *

State Key Laboratory of Supramolecular Structure and Materials, College of Chemistry, Jilin University, Changchun 130012, PR China

ARTICLE INFO

Article history:
Received 19 July 2011
Received in revised form 27 October 2011
Accepted 22 November 2011
Available online 17 December 2011

Keywords:
$Au^{I}\cdots Au^{I}$ interaction
Microwire
Vapor response
Photo response
Semiconductor

ABSTRACT

Organic semiconducting microwires can be self-assembled from a trinuclear gold(I) complex $Au^{I}_{3}(MeN{=}COMe)_{3}$ (Au_3A_3) based on extended intermolecular $Au^{I}\cdots Au^{I}$ interactions by a simple solution method. High mobility (0.23 $cm^2 V^{-1} s^{-1}$) of the microwires measured in ambient conditions by organic field-effect transistor (OFET) devices was achieved, vapor and photo responsive conductive characteristics with great sensibility, reversibility and rapid response were also revealed. The $Au^{I}\cdots Au^{I}$ interaction based structure of the Au_3A_3 microwires can broaden the scope of nano- and micro-scale organic semiconductors and will be valuable for the future design and synthesis of new organic semiconducting materials and also have potential in the fields of chemo-sensing and photo detectors.

1. Introduction

The interest in using organic and organometallic molecules to fabricate attractive one-dimensional (1D) crystalline building blocks such as nano/microwires or ribbons for applications in the fields of high performance electronics has grown significantly and much progress has been made [1–6]. These 1D materials are potential candidates in the fields including organic light-emitting diodes (OLEDs), organic field effect transistors (OFETs), photodetectors and solar cells, etc. [7–20]. Obviously finding out driving forces that can not only encourage the formation of nano/microsize 1D structures, but also lead to novel electronic characteristics has become an issue in general pursuit of an answer. Non-covalent intermolecular interactions such as H-bonding, $\pi\cdots\pi$ stacking, electrostatic and van der Waals interactions were widely used as efficient means in 1D molecular assemblies. Except for these traditional driving forces, some intermolecular weak metal–metal interactions such as $Pt^{II}\cdots Pt^{II}$ can also be employed in the construction of nano/micro 1D molecules [21–24]. It is obvious that these metal interaction based materials are expected to show outstanding conductive properties that have so far been sparsely documented [25–28]. Due to these weak metal interactions some 1D nano-structured materials showed external stimuli (such as chemical vapor and photo irradiation) responsive behaviors which may be useful in the fields of sensors and opto-electronic switching devices [29–31].

It has been demonstrated that the vacuum deposition process was an efficient approach to prepare high performance optical and electronic devices, however, this approach always involves multiple and complex steps, thereby increases manufacturing costs. Recently, much effort has been invested in developing organic nano/micro semiconducting materials that are suitable for simple device process techniques, with a view to reducing processing costs. Solution process has been demonstrated to be an important way for preparing low-cost and large-area integrated organic electronic devices. Therefore, it remains an important task to achieve solution produced 1D materi-

* Corresponding authors. Tel.: +86 431 85168484; fax: +86 431 85193421.
E-mail addresses: hongyuzhang@jlu.edu.cn (H. Zhang), yuewang@jlu.edu.cn (Y. Wang).

1566-1199/$ - see front matter © 2011 Elsevier B.V. All rights reserved.
doi:10.1016/j.orgel.2011.11.013

als and successfully apply them in the fabrication of high mobility OFET devices [32–35].

In this literature, we report the $Au^{I}\cdots Au^{I}$ interaction induced 1D microstructures of a gold complex $Au^{I}_{3}(MeN{=}COMe)_3$ (Au_3A_3) [36,37] (Fig. 1a) through a simple solution process as well as the semiconducting properties of the in situ formed microwires by fabricating field-effect transistors. Notably, the produced microwires exhibit interesting photo- and vapor-responsive conductive properties. Showing that it is possible to prepare high quality $Au^{I}\cdots Au^{I}$ based 1D crystals with field-effect charge carrier mobility and external stimuli responsive properties by solution process, which makes this material very interesting for potential applications in solution process electronics.

2. Experimental

2.1. Materials and device fabrication

Gold complex Au_3A_3 shows perfect solubility in many organic solvents. By taking advantage of this virtue, we succeeded in obtaining microstructures of these compounds through a simple drop-cast method using numerous solvents. *I–V* measurement was performed on Au_3A_3 microwires by a simple device: Au_3A_3 solution (dichloroethane, 2 mg/mL) was drop-cast and self-assembled on SiO_2 insulated substrates. Gold was deposited on top through a shadow mask to serve as electrodes (Supplementary Fig. S4). The lengths of the microwires were mostly larger than the electrode gaps (150 μm) so many of them were able to cross over the gap and connect the two gold electrodes. In order to measure the field-effect characteristics of the crystalline microwires, top-contact/bottom gate configuration OFET devices were fabricated. The OFET devices were prepared on a SiO_2 (300 nm thickness, capacitance $C \approx 11\ nFcm^{-2}$) dielectric layer with underlying doped silicon as the gate electrode. The SiO_2 surface was modified with *n*-octadecyltrichlorosilane (OTS). The microwires were prepared by drop-cast and slow volatilization method mentioned before on the substrate. Subsequently, gold was deposited on top of the microwires through a gold wire (diameter = 20 μm) shadow mask to form source and drain electrodes (the typical channel length was 15–20 μm). Photo and vapor responsive conducting property experiments were conducted on the Au_3A_3 microwires using a silver–palladium electrode (Supplementary Fig. S5). Au_3A_3 solution (dichloroethane, 2 mg/mL) was drop-cast and self-assembled on the electrodes to form microwires.

2.2. Characterization of the Au_3A_3 microwires and OFET measurements

Compound Au_3A_3 was synthesized according to known articles [36,37]. The microscopy images of as-prepared nano/microwires were obtained on an Olympus BX51 fluorescence microscope. FESEM images were achieved on a JSM 6700F field emission scanning electronic microscope. TEM images were performed on a Hitachi H-8100IV transmission electronic microscope. X-ray Diffraction was carried out on a Rigaku D/Max 2550 X-ray diffractometer. Photoluminescence spectra were recorded on a Perkin-Elmer LS 55 spectrophotometer. The *I–V* measurement was carried out after assembly on the electrode and the data was collected by an electrochemical workstation. Field effect mobilities of the Au_3A_3 microwires were measured by using a top contact OFET device. Au_3A_3 microwires were fabricated on a Si/SiO_2 (300 nm) substrate after being drop-cast and dried in air, source–drain electrodes (Au) were evaporated through gold wire (20 μm) shadow masks. The electrical characteristics were measured in ambient laboratory conditions by using a Keithley 2636A semiconductor analyzer. Average field effect mobility is calculated in the saturation regime using equation: $I_{DS} = \mu CW/2L\ (V_G - V_T)^2$ in which L is the channel length, W is the channel width which, C is the capacitance per unit area of the insulator layer, V_T is the threshold voltage and μ is the mobility in the saturation region [38].

3. Results and discussion

3.1. Microwire morphology and conductivity

Fig. 1b and d illustrates typical SEM spectroscopy images of Au_3A_3 microwires self-assembled on silicon substrates from tetrahydrofuran (THF, 2 mg/mL) and dichloroethane (2 mg/mL) solutions, respectively, using drop-cast method at room temperature. The images show uniform well-defined 1D micro/nanowires with diameters ranging from 100 to 1000 nm achieved from dichloroethane and 2000–3000 nm wires from THF, indicating changeable size nano/microwires could be obtained by changing solvents. Further morphology characterizations of the formed microwires from dichloroethane were performed on a transmission electron microscope and shown in Fig. 1f. Au_3A_3 microwires could also be achieved in numerous other solutions such as chloroform, chlorobenzene, and tetrachloroethane (Supplementary Fig. S1), demonstrating the generality of 1D self-assembly feature of this gold(I) complex.

It is well-known that the assembly morphologies of molecule based materials are often controlled by their intermolecular interactions. So the molecular packing characteristics of Au_3A_3 in the single crystals can provide useful information for the explanation of the 1D morphology in this study. Single crystals qualified for X-ray diffraction (XRD) were achieved by Balch and co-workers and crystal analysis revealed that Au_3A_3 crystallized as three polymorphs: hexagonal, triclinic and monoclinic, among which only the hexagonal polymorph could form needle shaped crystals. Based on the comparison of the XRD graphs of Au_3A_3 nano/microwires with the standard XRD graphs simulated from hexagonal polymorph crystals, it was demonstrated that the XRD pattern of the nano/microwires was nearly the same as that of hexagonal polymorph crystals. (Supplementary Fig. S2). Generally, nano/microcrystals displayed incomplete XRD peaks and different relative-diffraction-intensity compared with their corresponding powder samples. This was due to the fact that the crystal powder is isotropic and the nano/

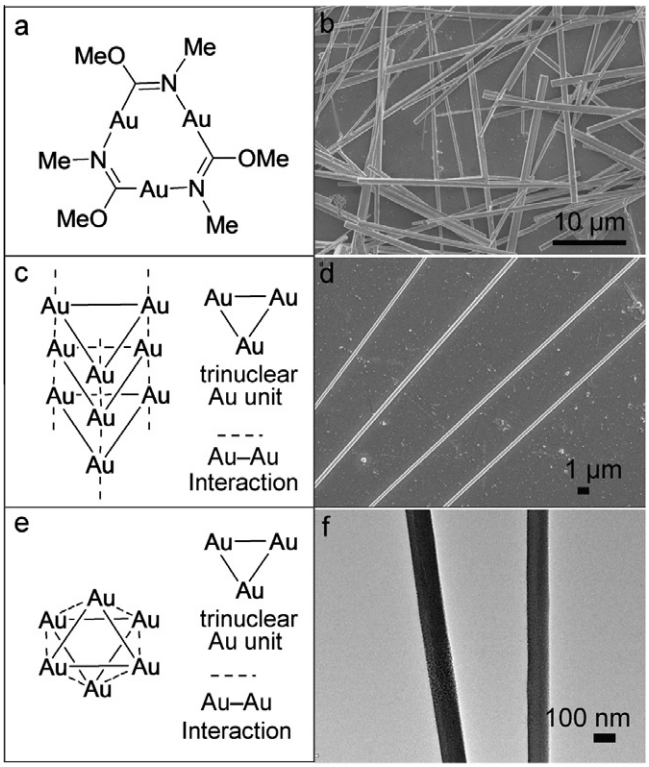

Fig. 1. (a) Molecular structure of compound Au_3A_3, (b) SEM images of Au_3A_3 microwires achieved from THF (2 mg/mL). (d) SEM and (f) TEM images of Au_3A_3 microwires achieved from dichloroethane (2 mg/mL). The two types of stacking in the hexagonal form of Au_3A_3: (c) prismatic and (e) offset.

microcrystals are not completely isotropic. This reveals that our Au_3A_3 nano/microwires have the exact packing feature of the hexagonal polymorph. To further confirm the phase property of the nano/microwires, their emission spectrum (Supplementary Fig. S3) has been recorded and exhibited identical profile compared with that of hexagonal polymorph crystals [39]. These results can support that the Au_3A_3 microwires are indeed packed in the hexagonal polymorph and are based upon $Au^I\cdots Au^I$ interactions. Balch and co-workers have thoroughly investigated the packing characteristics of the hexagonal polymorph crystals. In the crystal there are prismatic and disordered (offset by 60°) stacking modes and both stacks run parallel to the crystallographic c axis and are based on aurophilic interactions (Fig. 1c and e) [39,40].

It has been reported before that some weak metal interaction based complexes can be fabricated into nano or microsize materials which possess conductive properties [25–28]. Based on this information it is reasonable to suspect that the well-defined 1D Au_3A_3 microwires may be promising candidates for the fabrication of high performance electronic devices. To confirm our speculation we carried out direct current–voltage (I–V) measurement to detect the conductive characteristics of the Au_3A_3 microwires. The electric conductivity at the voltage of 10 V was as high as 0.1 μA per wire (Fig. 2). The excellent conductive properties of the Au_3A_3 microwires should arise from the 1D extended $Au^I\cdots Au^I$ interactions based on $5dz^{10}$ orbitals of Au^I ions along the microwires.

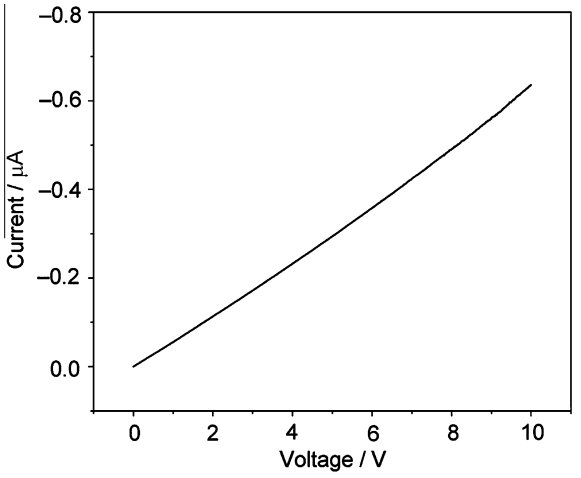

Fig. 2. I–V curves of Au_3A_3 microwires produced by solution process.

3.2. OFET device performance

The results achieved present Au_3A_3 as a good candidate for semiconducting materials. Fig. 3a and b shows the output and transfer characteristics of our fabricated OFET device based on solution processed 1D crystalline Au_3A_3 microwires, in which a clear effect of the gate on the current was observed. Only p-channel activity is observed

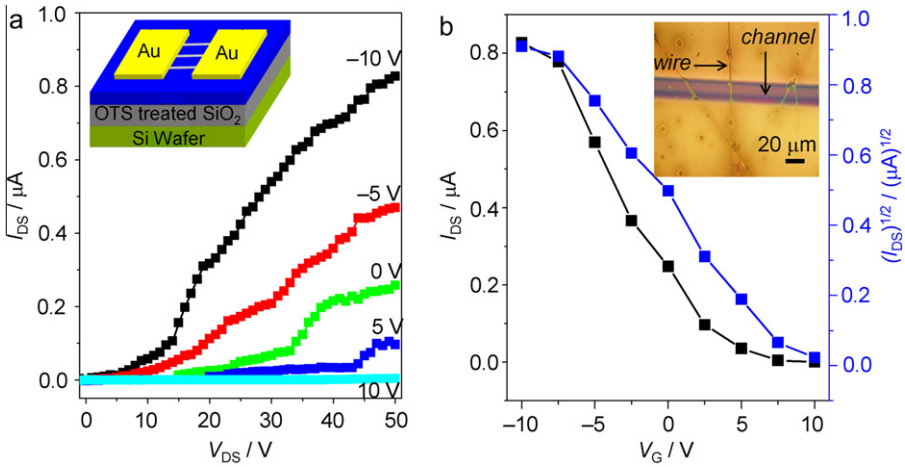

Fig. 3. Field-effect characteristics of the OFET based on Au_3A_3 microwires: typical (a) output characteristics (inset: Schematic illustration of the Au_3A_3 microwire OFET device) and (b) transfer characteristics (inset: optical microscopy image of the Au_3A_3 micro-transistor).

from the device, indicating holes are the major charge carriers in the conducting channel.

More than 10 devices were tested with hole mobilities from 0.15 to 0.23 $cm^2 V^{-1} s^{-1}$, threshold from 20 to 10 V, and I_{on}/I_{off} of about 10^3. The performances of the transistors were very stable and highly reproducible in air. However from the output characteristics we can see at low drain voltage there are signals of contact resistance; this might be due to the ineffective contact between the microwires and the drain/source electrodes. Also, the on/off ratio is low due to the large off current, as observed in Fig. 3b. This may be associated with the remaining conductive paths on the surface of the crystals, which might have been created during the drying process of the crystals after re-crystallization by solution process [41].

3.3. Photo and vapor responsive conductive properties

Reports lately confirm that some weak metal–metal interaction based 1D micro-structured materials possess vapor and photo responsive conductive properties [42]. The conductivity of the Au_3A_3 microwires is due to the $Au^I \cdots Au^I$ interactions, therefore there is a reason to believe Au_3A_3 microwires may possess similar stimuli-responsive conducting properties. In order to verify our hypothesis, we conducted conductivity measurements of Au_3A_3 microwires under certain excitation wavelengths and different solvent atmospheres.

The photo-responsive characteristics of Au_3A_3 microwires show photoswitch performance, as presented in Fig. 4a. The devices were capable of switching on/off reversibly and rapidly upon exposure to pulsed incident light. Fig. 4b shows a series of current responses of the Au_3A_3 microwire based sensor to dynamic switches of different light intensities. When the sensor device was exposed to a light with the intensity of 42 $\mu W/cm^2$, the current promptly increased and then gradually reached a relatively stable value. When the light was switched off again, the current abruptly decreased and rapidly reached another relatively stable value. The same procedure was repeated with lights of various intensities and showed the current response increased from low to high light intensities. The response and recovery time (defined as the time required reaching 90% of the final equilibrium value) were around 20 s and 15 s, respectively. The reason for the photoswitch effect should be attributed to the photo-induced carrier in the Au_3A_3 microwires, which gives a net increase in the concentration of the charges, therefore enhancing the electrical conductivity.

The exposure of some vapor volatile organic compounds (VOC) to Au_3A_3 nano/microwires also resulted in changes of conducting properties as we expected. Testing procedures carried out provided more information on three of the most important parameters for a sensing device: sensitivity, response time and reproducibility. Fig. 5a depicts the vapor response properties of the Au_3A_3 microwires. The sample was exposed to an alternating atmosphere of nitrogen with or without organic vapor. Upon introduction of ethanol vapor (2.5 mmol/L) by a nitrogen flow of 300–400 $cm^3 min^{-1}$, the conductivity increased substantially. After removing the ethanol vapor by purging with 100% nitrogen, the conductivity decreases and recovers to the initial level again (Fig. 5a). The response and recovery time were about 25 s and 15 s, respectively, and the sensitivity I_{on}/I_{off} was approximately 100–120. We note that the conductivity of the Au_3A_3 microwires show a relative response (Fig. 5b) and good linearity (Fig. 5c) with the concentration of ethanol, clearly showing the introduction of ethanol is the reason of the conductivity increase. The responsive properties can be repeated without obvious deviation for many cycles, indicative of an excellent reversibility, and all experiments were carried out at room temperature and ambient atmosphere conditions. Ten other organic vapors have been employed to check the responsive selectivity of these microwires, only methanol (Supplementary Fig. S6a) and acetonitrile (Supplementary Fig. S6b) display a similar response to ethanol vapor, the others such as THF, acetone, benzene and so on do not induce the change of conductivity (Fig. 5d). Therefore, the vapor responsive conducting properties of the Au_3A_3 microwires exhibited certain selectivity. Our previous reports show that the intermolecular interactions

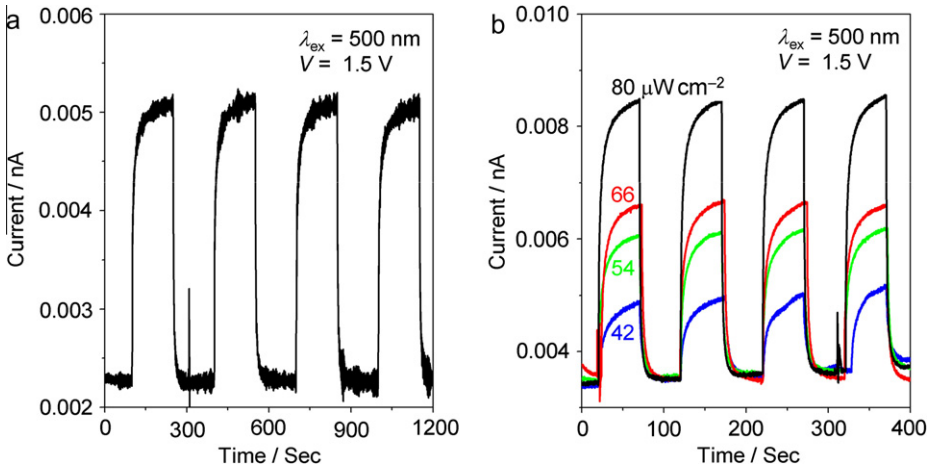

Fig. 4. (a) Current response of Au_3A_3 microwires which can be switched on/off rapidly by photo irradiation. (b) Current response results of Au_3A_3 microwires to different intensities of photo irradiation.

caused by VOC guests may affect the metal–metal distance coupled by changing the energy gap and lead to slight variations in the coordination bond angles which are crucial regarding the charge transfer [24,42]. In this case, ethanol

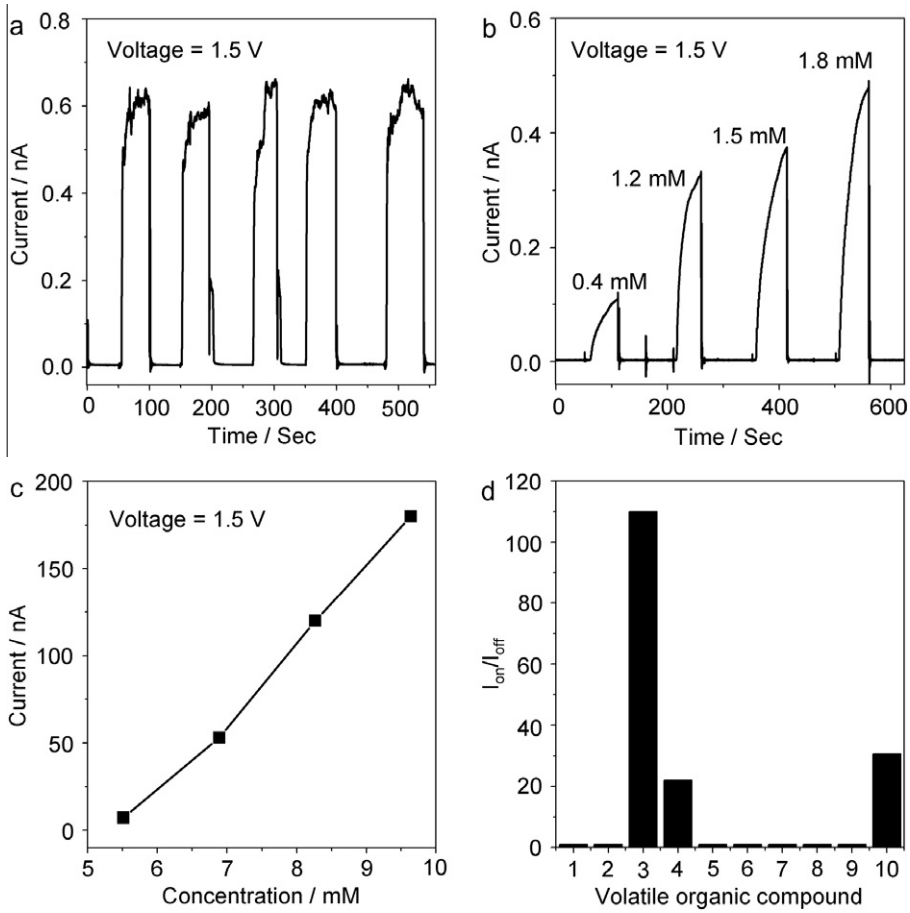

Fig. 5. (a) Current response of Au_3A_3 microwires which can be switched on/off by introducing ethanol (2.5 mmol/L) by a nitrogen flow at room temperature under a constant voltage (1.5 V). (b) Current response results of Au_3A_3 microwires to different concentrations of ethanol. (c) Linear dependence between response current and ethanol concentration. (d) Sensitivity (I_{on}/I_{off}) of Au_3A_3 microwires to various organic vapors: (1) THF, (2) benzene, (3) ethanol, (4) methanol, (5) acetone, (6) propyl alcohol, (7) xylene, (8) butanol, (9) pentanol, (10) acetonitrile.

molecules may contact with the Au_3A_3 wires based on hydrogen bond interactions and result in the variation of conductivity.

4. Conclusions

In summary we have demonstrated that crystalline, semiconducting microwires can be self-assembled from a trinuclear gold complex Au_3A_3 based on extended intermolecular $Au^I \cdots Au^I$ interactions by a simple solution process. The formed microwires exhibiting excellent electrical conductivity properties as well as high hole mobility ($0.23\ cm^2\ V^{-1}\ s^{-1}$) suggest they are potential candidates for the development of high performance semiconducting devices. The $Au^I \cdots Au^I$ interaction based structure of the Au_3A_3 microwires can also broaden the scope of nano- and micro-scale organic semiconductors and will be valuable for the future design and synthesis of new organic semiconducting materials. Vapor and photo responsive conductive characteristics with good sensibility, reversibility and rapid response were also revealed, suggesting that Au_3A_3 microwires have potential in the fields of chemosensing and photo detectors.

Acknowledgments

This work was supported by the National Natural Science Foundation of China (50773027, 50733002 and 51173067), the Major State Basic Research Development Program (2009CB939700), and 111 Project (B06009).

Appendix A. Supplementary data

Supplementary data associated with this article can be found, in the online version, at doi:10.1016/j.orgel.2011.11.013.

References

[1] V.C. Sundar, J. Zaumseil, V. Podzorov, E. Menard, R.L. Willet, T. Someya, M.E. Gershenson, J.A. Rogers, Elastomeric transistor stamps: reversible probing of charge transport in organic crystals, Science 303 (2004) 1644.
[2] Q. Niu, Y. Zhou, L. Wang, J. Peng, J. Wang, J. Pei, Y. Cao, Enhancing the performance of polymer light-emitting diodes by integrating self-assembled organic nanowires, Adv. Mater. 20 (2008) 964.
[3] Y. Che, X. Yang, S. Loser, L. Zang, Expedient vapor probing of organic amines using fluorescent nanofibers fabricated from an n-type organic semiconductor, Nano Lett. 8 (2008) 2219.
[4] H. Xin, F.S. Kim, S.A. Jenekhe, Highly efficient solar cells based on poly(3-butylthiophene) nanowires, J. Am. Chem. Soc. 130 (2008) 5424.
[5] K. Huang, Y. Hsiao, W. Whang, Low-temperature formation of self-assembled 1,5-diaminoanthraquinone nanofibers: substrate effects and field emission characteristics, Org. Electron. 12 (2011) 686–693.
[6] M. Ichikawa, T. Kato, T. Uchino, T. Tsuzuki, M. Inoue, Thin-film and single-crystal transistors based on a trifluoromethyl-substituted alternating (thiophene/phenylene)-co-oligomer, Org. Electron. 11 (2010) 1549–1554.
[7] T. Naddo, Y. Che, W. Zhang, K. Balakrishnan, X. Yang, M. Yen, J. Zhao, J.S. Moore, L. Zang, Detection of explosives with a fluorescent nanofibril film, J. Am. Chem. Soc. 129 (2007) 6978.
[8] Y. Che, A. Datar, K. Balakrishnan, L. Zang, Ultralong nanobelts self-assembled from an asymmetric perylene tetracarboxylic diimide, J. Am. Chem. Soc. 129 (2007) 7234.
[9] O.J. Dautel, G. Wantz, R. Almairac, D. Flot, L. Hirsch, J.-P. Lere-Porte, J.-P. Parneix, F.S. Spirau, L. Vignau, J.J.E. Moreau, Nanostructuration of phenylenevinylenediimide-bridged silsesquioxane: from electroluminescent molecular J-aggregates to photoresponsive polymeric H-aggregates, J. Am. Chem. Soc. 128 (2006) 4892.
[10] Y.S. Zhao, C. Di, W. Yang, G. Yu, Y. Liu, J. Yao, Photoluminescence and electroluminescence from tris(8- hydroxyquinoline)aluminum nanowires prepared by adsorbent-assisted physical vapor deposition, Adv. Funct. Mater. 16 (2006) 1985.
[11] Y.S. Zhao, H. Fu, F. Hu, A. Peng, W. Yang, J. Yao, Tunable emission from binary organic one-dimensional nanomaterials: an alternative approach to white-light emission, Adv. Mater. 20 (2008) 79.
[12] A.L. Briseno, S.C.B. Mannsfeld, S.A. Jenekhe, Z. Bao, Y. Xia, Introducing organic nanowire transistors, Mater. Today 11 (2008) 38.
[13] A.L. Briseno, S.C.B. Mannsfeld, C. Reese, X. Lu, Y. Xiong, S.A. Jenekhe, Z. Bao, Y. Xia, Fabrication of field-effect transistors from hexathiapentacene single-crystal nanowires, Nano Lett. 7 (2007) 668.
[14] Q. Tang, H. Li, M. He, W. Hu, C. Liu, K. Chen, C. Wang, C. Liu, D. Zhu, Low threshold voltage transistors based on individual single-crystalline submicrometer-sized ribbons of copper phthalocyanine, Adv. Mater. 18 (2006) 65.
[15] L. Jiang, H. Dong, W. Hu, Organic single crystal field-effect transistors: advances and perspectives, J. Mater. Chem. 20 (2010) 4994.
[16] R. Li, W. Hu, Y. Liu, D. Zhu, Micro- and nanocrystals of organic semiconductors, Acc. Chem. Res. 43 (2010) 529.
[17] K. Takazawa, Y. Kitahama, Y. Kimura, G. Kido, Optical waveguide self-assembled from organic dye molecules in solution, Nano Lett. 5 (2005) 1293.
[18] F. Quochi, F. Cordella, A. Mura, G. Bongiovanni, F. Balzer, H.-G. Rubahn, Gain amplification and lasing properties of individual organic nanofibers, Appl. Phys. Lett. 88 (2006) 041106.
[19] Y.S. Zhao, J. Xu, A. Peng, H. Fu, Y. Ma, L. Jiang, J. Yao, Optical waveguide based on crystalline organic microtubes and microrods, Angew. Chem., Int. Ed. 47 (2008) 7301.
[20] Y.S. Zhao, A. Peng, H. Fu, Y. Ma, J. Yao, Nanowire waveguides and ultraviolet lasers based on small organic molecules, Adv. Mater. 20 (2008) 1661.
[21] A.L.F. Chow, M.H. So, W. Lu, N. Zhu, C.M. Che, Synthesis, photophysical properties, and molecular aggregation of gold(I) complexes containing carbon-donor ligands, Chem. Asian J. 6 (2011) 544.
[22] M. Enomoto, A. Kishimura, T. Aida, Coordination metallacycles of an achiral dendron self-assemble via metal–metal interaction to form luminescent superhelical fibers, J. Am. Chem. Soc. 123 (2001) 5608.
[23] W. Lu, V.A.L. Roy, C.M. Che, Self-assembled nanostructures with tridentate cyclometalated platinum(II) complexes, Chem. Commun. 38 (2006) 3972.
[24] Y. Sun, K. Ye, H. Zhang, J. Zhang, L. Zhao, B. Li, G. Yang, B. Yang, Y. Wang, S.W. Lai, C.M. Che, Luminescent one-dimensional nanoscale materials with $Pt^{II} \cdots Pt^{II}$ interactions, Angew. Chem., Int. Ed. 45 (2006) 5610.
[25] A. Kobayashi, T. Kojima, R. Ikeda, H. Kitagawa, Synthesis of a one-dimensional metal-dimer assembled system with interdimer interaction, M2(dtp)4 (M = Ni, Pd; dtp = dithiopropionato), Inorg. Chem. 45 (2006) 322.
[26] M.Y. Yuen, V.A.L. Roy, W. Lu, S.C.F. Kui, G.S.M. Tong, M.H. So, S.S.Y. Chui, M. Muccini, J.Q. Ning, S.J. Xu, C.M. Che, Semiconducting and electroluminescent nanowires self-assembled from organoplatinum(II) complexes, Angew. Chem., Int. Ed. 47 (2008) 9895.
[27] Y. Chen, K. Li, W. Lu, S.S.Y. Chui, C.W. Ma, C.M. Che, Photoresponsive supramolecular organometallic nanosheets induced by $Pt^{II} \cdots Pt^{II}$ and $C–H \cdots \pi$ interactions, Angew. Chem., Int. Ed. 48 (2009) 9909.
[28] C.M. Che, C.F. Chow, M.Y. Yuen, V.A.L. Roy, W. Lu, Y. Chen, S.S.Y. Chui, N. Zhu, Single microcrystals of organoplatinum(II) complexes with high charge-carrier mobility, Chem. Sci. 2 (2011) 216.
[29] X. Zhang, J. Jie, W. Zhang, C. Zhang, L. Luo, Z. He, X.H. Zhang, W. Zhang, C. Lee, S. Lee, Photoconductivity of a single small-molecule organic nanowire, Adv. Mater. 20 (2008) 2427.
[30] J. Yoon, S.K. Chae, J.M. Kim, Colorimetric sensors for volatile organic compounds (VOCs) based on conjugated polymer-embedded electrospun fibers, J. Am. Chem. Soc. 129 (2007) 3038.
[31] A. Kishimura, T. Yamashita, T. Aida, Phosphorescent organogels via "Metallophilic" interactions for reversible RGB-color switching, J. Am. Chem. Soc. 127 (2005) 179.
[32] D.H. Kim, D.Y. Lee, H.S. Lee, W.H. Lee, Y.H. Kim, J.I. Han, K. Cho, High-mobility organic transistors based on single-crystalline microribbons of triisopropylsilylethynyl pentacene via solution-phase self-assembly, Adv. Mater. 19 (2007) 678.

[33] Y. Chen, K. Li, H.O. Lloyd, W. Lu, S.S.Y. Chui, C.M. Che, Tetrakis(arylisocyanide) rhodium(I) salts in water: NIR luminescent and conductive supramolecular polymeric nanowires with hierarchical organization, Angew. Chem., Int. Ed. 49 (2010) 9968.
[34] J.H. Oh, H.W. Lee, S. Mannsfeld, R.M. Stoltenberg, E. Jung, Y.W. Jin, J.M. Kim, J.-B. Yoo, Z. Bao, Solution-processed, high-performance n-channel organic microwire transistors, Proc. Natl. Acad. Sci. USA 106 (2009) 6065.
[35] W. Jiang, Y. Zhou, H. Geng, S. Jiang, S. Yan, W. Hu, Z. Wang, Z. Shuai, J. Pei, Solution-processed, high-performance nanoribbon transistors based on dithioperylene, J. Am. Chem. Soc. 133 (2011) 1.
[36] J.E. Parks, A.L. Balch, Gold carbene complexes: preparation, oxidation, and ligand displacement, J. Organomet. Chem. 71 (1974) 453.
[37] G. Minghetti, F. Bonati, Trimeric (alkoxy)(alkylimino)methylgold(I) compounds, $[(RO)(R'N{=})CAu]_3$, Inorg. Chem. 13 (1974) 1600.
[38] G. Horowitz, Organic field-effect transistors, Adv. Mater. 10 (1998) 365.
[39] R.L. White-Morris, M.M. Olmstead, S. Attar, A.L. Balch, Intermolecular interactions in polymorphs of trinuclear gold(I) complexes: insight into the solvoluminescence of $Au_I^3(MeN{=}COMe)_3$, Inorg. Chem. 44 (2005) 5021.
[40] J.C. Vickery, M. Olmstead, E.Y. Fung, A.L. Balch, Solvent-stimulated luminescence from the supramolecular aggregation of a trinuclear gold(I) complex that displays extensive intermolecular Au–Au interactions, Angew. Chem., Int. Ed. 36 (1997) 1197.
[41] Y. Takahashi, T. Hasegawa, S. Horiuchi, R. Kumai, Y. Tokura, G. Saito, High mobility organic field-effect transistor based on hexamethylenetetrathiafulvalene with organic metal electrodes, Chem. Mater. 19 (2007) 6382.
[42] Y. Zhang, H. Zhang, X. Mu, S.W. Lai, B. Xu, W. Tian, Y. Wang, C.M. Che, Photo- and vapor-responsive conducting microwires based on Pt–Pt interactions, Chem. Commun. 41 (2010) 7727.